ISSN 1674-1056
http://cpb.iphy.ac.cn
http://iopscience.iop.org/cpb
中国物理 B
Chinese Physics
中国物理
Chinese Physics B

Time-dependent first-principles study of optical response of $BaTiO_3$ quantum dots coupled with silver nanowires

Bo-Xun Han(韩博逊), Hong Zhang(张红)

Citation: Chin. Phys. B . 2019, 28(6): 067301. **doi:** 10.1088/1674-1056/28/6/067301
Journal homepage: http://cpb.iphy.ac.cn; http://iopscience.iop.org/cpb

What follows is a list of articles you may be interested in

Subwavelength asymmetric Au-VO_2 nanodisk dimer for switchable directional scattering

Han-Mou Zhang(张汉谋), Wu-Yun Shang(尚武云), Hua Lu(陆华), Fa-Jun Xiao(肖发俊), Jian-Lin Zhao(赵建林)
Chin. Phys. B . 2018, 27(11): 117301. **doi:** 10.1088/1674-1056/27/11/117301

Selective enhancement of green upconversion luminescence of Er-Yb: $NaYF_4$ by surface plasmon resonance of $W_{18}O_{49}$ nanoflowers and applications in temperature sensing

Ang Li(李昂), Jin-Lei Wu(吴金磊), Xue-Song Xu(许雪松), Yang Liu(刘洋), Ya-Nan Bao(包亚男), Bin Dong(董斌)
Chin. Phys. B . 2018, 27(9): 097301. **doi:** 10.1088/1674-1056/27/9/097301

Novel hole transport layer of nickel oxide composite with carbon for high-performance perovskite solar cells

Sajid, A M Elseman, Jun Ji(纪军), Shangyi Dou(窦尚轶), Hao Huang(黄浩), Peng Cui(崔鹏), Dong Wei(卫东), Meicheng Li(李美成)
Chin. Phys. B . 2018, 27(1): 017305. **doi:** 10.1088/1674-1056/27/1/017305

Optical interaction between one-dimensional fiber photonic crystal microcavity and gold nanorod

Yang Yu(于洋), Ting-Hui Xiao(肖廷辉), Zhi-Yuan Li(李志远)
Chin. Phys. B . 2018, 27(1): 017301. **doi:** 10.1088/1674-1056/27/1/017301

Tunable multiple plasmon resonances and local field enhancement of nanocrescent/nanoring structure

Wang Bin-Bing, Zhou Jun, Chen Dong, Fang Yun-Tuan, Chen Ming-Yang
Chin. Phys. B . 2015, 24(8): 087301. **doi:** 10.1088/1674-1056/24/8/087301

Time-dependent first-principles study of optical response of $BaTiO_3$ quantum dots coupled with silver nanowires*

Bo-Xun Han(韩博逊)[1], and Hong Zhang(张红)[1,2,†]

[1] College of Physical Science and Technology, Sichuan University, Chengdu 610065, China
[2] Key Laboratory of High Energy Density Physics and Technology (Ministry of Education), Sichuan University, Chengdu 610065, China

(Received 14 January 2019; revised manuscript received 29 March 2019; published online 8 May 2019)

All-inorganic perovskite quantum dots (QDs) have drawn much attention due to their prominent quantum-size effects and highly tunable optical properties. Tuning the size of perovskite QDs is attractive for many potential applications. For instance, smaller QDs exhibit more evident quantum properties than larger QDs, but present a blue-shifted spectrum, which limits their applications. Here, we conduct a systematically theoretical analysis about the optical response and plasmon resonance of comparatively small barium titanate quantum dots (BTO–QDs) coupled with silver (Ag) nanowires based on time-dependent density functional theory (TDDFT). Our results show that the silver nanowires can induce an intense optical response respectively in the infrared and visible region to eliminate the spectrum-shift. Furthermore, the absorption spectrum and plasmon resonance can be effectively modified by either altering the position of the silver nanowires or changing the thickness of the BTO–QDs. More importantly, these two methods can act simultaneously, this maybe provide a new approach to implementing the quantum control.

Keywords: perovskite, QDs, TDDFT, plasmon resonance

PACS: 73.20.Mf, 73.21.–b **DOI:** 10.1088/1674-1056/28/6/067301

1. Introduction

All-inorganic perovskite structures have attracted much attention due to their excellent photoelectric properties such as superconductivity, above-band gap photovoltage and spin-dependent transport.[1–10] For instance, strontium niobate, a kind of all-inorganic perovskite structure, has a proper bandgap and hydrogen standard electrode potential.[11,12] It shows great potential applications in photocatalysis and has recently become a hot research topic. Quantum dots (QDs) are tiny semiconductor nanoparticles, normally only 2 nm–20 nm in diameter, their optical and electronic properties differ from their bulk phases. The size-dependent quantum effects of QDs are attractive to many potential applications.[13] For example, larger QDs have greater red-shift and stronger absorption in the absorption spectrum than smaller QDs, and *vice versa*. The size-dependent absorption and highly efficient light emission in QDs are particularly suitable for optical communication technologies and manufacturing high-performance photovoltaic devices, as well as light absorbers in photocatalysis.[14–19] Owing to their high extinction coefficients and tunable absorption spectrum, QDs are proper candidates for reducing the cost and increasing the efficiency of photocells we are using today. Perovskite QDs inherit all the above-mentioned advantages of both perovskite structures and QDs' structures, which makes them promising materials.[20–23] Despite many advantages, there are still some defects in perovskite QDs due to the limitations of the QD structure itself. For instance, we cannot achieve strong absorption and strong quantum effects at the same time.

For this case, recently, a kind of hybrid structure comprised of QDs and nanowires has become a hot topic both theoretically and experimentally.[24–27] The morphology of the nanowire allows the electrons to have a direct pathway to the photoanode. On the other hand, some noble metal nanowires can provide an extra electric field under an external field due to their ultrahigh charge mobilities, and hence strengthening the light absorption of the whole system. Consequently, a strong absorption intensity can be obtained without reducing the quantum effect. In this work, barium titanate quantum dots (BTO–QDs) coupled with silver nanowires (BTO–QDs/Ag) are studied based on the time-dependent density functional theory (TDDFT), and the influence of the coupling silver nanowires is explicitly investigated. Our study shows that the optical response and photoelectric properties of BTO–QDs/Ag hybrid system can be effectively modified by either changing the position of the silver nanowires or thickening the BTO–QDs.

The rest of this paper is organized as follows. In Section 2, we describe the computational details involved in this paper. Then in Section 3, we compare the BTO–QDs/Ag hybrid structures with the separate BTO–QDs to elucidate the advantages and necessity of adding silver nanowires (in Subsection 3.1), the absorption spectrum and plasmons in rotated

*Project support by the National Key Research and Development Program of China (Grant No. 2017YFA0303600) and the National Natural Science Foundation of China (Grant No. 11474207).

†Corresponding author. E-mail: hongzhang@scu.edu.cn

© 2019 Chinese Physical Society and IOP Publishing Ltd

$2 \times 2 \times 1$ BTO–QDs/Ag hybrid structure to observe the effects of rotation on the system (in Subsection 3.2) those phenomena in thickened $2 \times 2 \times 2$ BTO–QDs/Ag system to observe the effects of thickening, and discuss those phenomena in rotated thickened $2 \times 2 \times 2$ BTO–QDs/Ag hybrid structure to investigate the results of the two operations acting on the system together(in Subsection 3.4. Finally, in Section 4, we draw some conclusions from our results.

2. Computational details

All our calculations are performed by using the real-space and real-time density functional theory (TDDFT) approach as employed in the OCTOPUS code.[28] The BTO–QDs and silver nanowires are described by the Hartwigsen–Goedecker–Hutter pseudopotentials. The generalized gradient approximation (GGA) expressed by the Perdew–Burke–Ernzerhof (PBE) functional for the exchange–correlation is used for calculating both the ground state and excited state.[29,30] The system is excited by a functional impulse which describes the perturbation of the total density of the system to obtain the linear optical absorption spectrum along a specific direction. The induced charge density distributions are extracted by the Fourier transformation of the dipole strength. The simulation box is constructed by adding spheres created around each atom with a radius of 6 Å and a uniform mesh grid of 0.3 Å. Approximated enforced time-reversal symmetry (AETRS) algorithm is used to approximate the evolution operator in our real-time propagation, and the Kohn-Sham wave functions are evolved for typically 6000 steps in time steps of 0.005 $\hbar$/eV $\approx$ 0.0033 fs.

3. Results and discussion

3.1. Comparison between separate BTO–QDs' system and BTO–QDs/Ag hybrid system

As many studies proved that combining the silver nanowires with materials can strengthen optical properties or even induce a lot of novelties,[24–27] for comparison, two different sized BTO–QDs along with their respective hybrid systems are taken into account. Figure 1 shows a top view and a side view for each of these four structures and their geometric parameters.

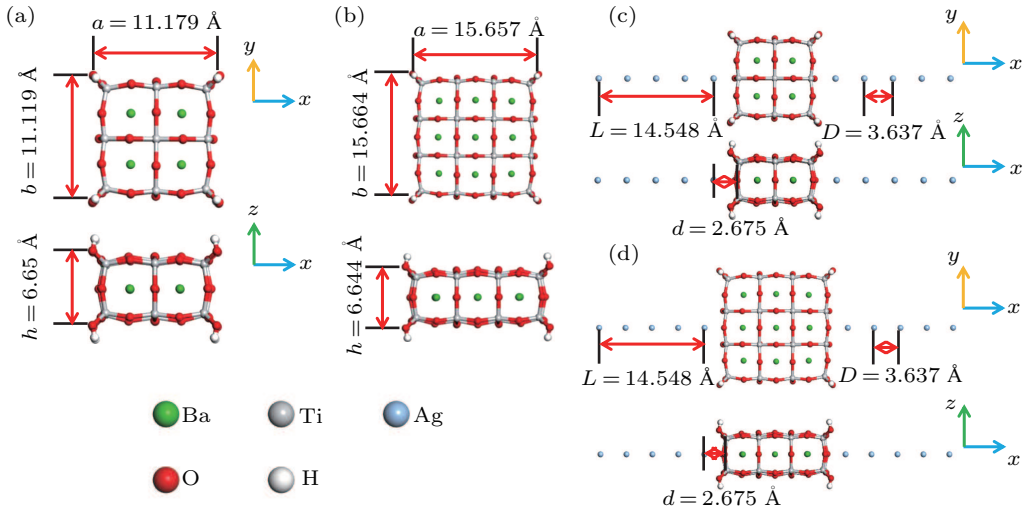


Fig. 1. Top view and side view of (a) $2 \times 2 \times 1$ BTO–QDs, (b) $3 \times 3 \times 1$ BTO–QDs, (c) $2 \times 2 \times 1$ BTO–QDs/Ag, and (d) $3 \times 3 \times 1$ BTO–QDs/Ag hybrid system, with red, green, white, silver, and blue balls denoting oxygen, barium, hydrogen, titanium, and silver atoms, respectively.

As plotted in Figs. 1(c) and 1(d), the nanowire parameters of two sized hybrid systems are all the same. In these systems, the silver nanowire lies in the Ba–O plane along the x axis, and the Ba–O plane is set to be $z = 0$. The distance between the terminal silver ion and its nearest oxygen atom is 2.675 Å, while the spacing between two silver ions is 3.637 Å, and the length of silver nanowires is 14.548 Å. We first perform the DFT calculations to obtain their ground-states and then use the resulting electron distribution for calculating the next excited-states with the excitation pulse polarized in x-axis direction. Figures 2(a) and 2(b) present the optical absorption strength of the separate BTO–QDs along with their hybrid systems for an impulse excitation polarized in the x direction (along the silver nanowire direction), moreover, optical absorption strengths of the silver nanowires are also plotted in these two figures for comparison. The optical absorption spectra of the BTO–QDs and the corresponding hybrid system are generally analogous in the high-energy zone (2 eV–6 eV), while the situation is different in the low-energy zone (0 eV–2 eV). New absorption peaks emerge from the near-infrared region, and the main peaks have a much wider absorption range than the peaks of silver nanowire in the low-energy area, though the relative absorption strength drops by a factor of two as shown in Figs. 2(a) and 2(b). The silver nanowires serve as optical antennas, which effectively widen the absorption range of the hybrid systems to the low-energy region (0 eV–2 eV), for the

absorption strengths of the two sized BTO–QDs in 0 eV–2 eV are both negligible. After the coupling with silver nanowires, the absorption strength of hybrid systems is considerable no matter whether it is in ultraviolet, infrared, or the visible region, which implies the potential application in the euryphotic photosensitive detector. Besides, the main absorption peak of the hybrid system is closely related to the eigenfrequency of silver nanowire. Interestingly, the silver nanowires induced absorbing ranges (for about 0 eV–2 eV) of both hybrid structures split into two regions (*i.e.*, about 0 eV–0.5 eV and 0.5 eV–2 eV). We suppose that the main reason for this phenomenon is that the QDs are so small that the quantum confinement effects can make a sense in which the electrons cannot escape from the 'dot', thus allowing particle-in-a-box approximations to be adopted.[31] The behavior of electrons can be described by three-dimensional particle-in-a-box energy quantization equations. The solutions of above-mentioned equations have an important feature that when two or more of the lengths are the same, there are multiple wavefunctions corresponding to the same total energy. In our case, the length of '*a*' and the length of '*b*' are almost equivalent, so the separate BTO–QDs show twofold degeneracy. While the twofold degeneracy is broken when the silver nanowire is added into the system, which brings on the split phenomena.

To explore these phenomena, the induced charge density distributions for these four structures at their absorbing peaks are calculated. Figures 2(c)–2(h) show the Fourier transformations of the induced charge density distributions. The induced charge density distributions of the two sized separate BTO–QDs at their respective energy resonance points (4.07 eV for $2\times2\times1$ and 4.97 eV for $3\times3\times1$) are shown in Figs. 2(c) and 2(d). Those of hybrid systems at the corresponding resonance points (4.06 eV for $2\times2\times1$ BTO–QDs/Ag and 4.96 eV for $3\times3\times1$ BTO–QDs/Ag) are presented in Figs. 2(f) and 2(h). The induced charge density distributions of the two sized hybrid system at their main peaks (1.12 eV for $2\times2\times1$ BTO–QDs/Ag and 1.17 eV for $3\times3\times1$ BTO–QDs/Ag) are depicted in Figs. 2(e) and 2(g), respectively. In Figs. 2(c) and 2(d), the induced charge intricately scattered all over the excited plane, and even a few plasmon resonance phenomena can be found. While in Figs. 2(f) and 2(h), the induced charge distributions within the $BaTiO_3$ (BTO) region of two sized hybrid systems at their corresponding resonance point are much more regular, but the oscillation phenomena of the silver nanowires are not so clear. In contrast, in Figs. 2(e) and 2(g), the collective oscillation phenomena are found in both BTO–QDs and silver nanowires. Furthermore, the charge distributions are more concentrated and present anti-symmetry. All the phenomena mentioned above prove that the silver nanowires can provide an extra electric field, and hence strengthen the optical properties of BTO–QDs in not only the low-energy range but also the high-energy range, and the silver nanowires play a key role in the collective oscillation phenomenon. Considering that the smaller QDs have the stronger quantum-size effects, the $2\times2\times1$BTO–QDs coupled with silver nanowires are chosen for the following research.

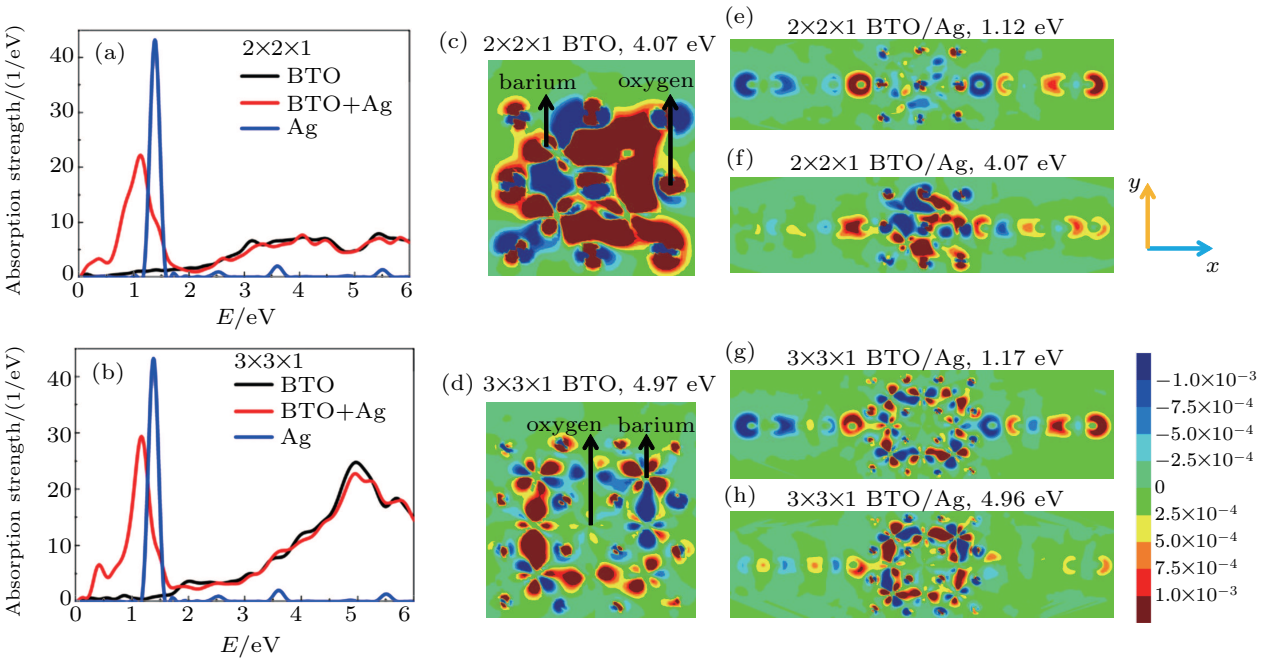


Fig. 2. Linear response (optical absorption) of (a) $2\times2\times1$ BTO–QDs, $2\times2\times1$ BTO–QDs/Ag, and silver nanowire. (b) Linear response (optical absorption) of $3\times3\times1$ BTO–QDs, $3\times3\times1$ BTO–QDs/Ag, and silver nanowire. Impulse excitation polarized in *x*-axis direction. Fourier transformations of the induced charge density distribution in the Ba–O plane ($z=0$ plane) at resonance point of (c) 4.07 eV for $2\times2\times1$ BTO, (d) 4.97 eV for $3\times3\times1$ BTO, (e) 1.12 eV for $2\times2\times1$ BTO/Ag, (f) 4.07 eV for BTO/Ag, (g) 1.17 eV for $3\times3\times1$ BTO/Ag, and (h) 4.96 eV for $3\times3\times1$ BTO/Ag, respectively.

3.2. Absorption spectrum and plasmons of rotated BTO–QDs/Ag system

Various excitation pulse polarized directions are always used to study optical response properties of materials, both experimentally and theoretically.[32–34] Here, as shown in Fig. 3(a), with a rotation of 45 degrees with respect to the Z axis, we obtain the rotated BTO–QDs (R-BTO), and the silver nanowire lies in the Ba–O plane along the x axis (diagonal direction). In this hybrid system, the geometric parameters are all the same as those in Fig. 1. Figure 3(b) shows the optical absorption spectrum of the R-BTO/Ag hybrid system (red curve) when the excitation light goes along the x axis direction (diagonal direction). Besides, the spectrum of Ag nanowires (blue curve) and the original BTO/Ag hybrid structure (black curve) are also plotted for comparison. Figure 3(b) clearly displays the redshift of the absorption region and the amplification of the absorption strength after the rotation, which implies its potential applications in photosensitive devices. It is noteworthy that the relative absorption strength of the main peak is twice as great as the original BTO/Ag system, even slightly higher than the strength of silver nanowire, which implies that the rotated pattern has a stronger excitation feature. This is because the perturbation field we used is a linear gradient field that the intensity of the excitation will increase with increasing the number of atoms passing through it.[35,36] Furthermore, a new peak appears in the visible light region at 1.72 eV, and a less obvious peak, of which the frequency is very close to that of silver nanowire, emerges at 1.41 eV.

The induced charge density distributions at three resonance points (0.84 eV, 1.72 eV, and 1.41 eV) of R-BTO/Ag system are shown in Figs. 3(c)–3(e). As we expected, the strong resonance phenomenon is found in both R-BTO and silver nanowire at the main peak (0.84 eV) as shown in Fig. 3(c). According to the dipole interaction theory,[37] at this resonance energy point, the hybrid system forms mutually attracted dipoles along the excitation direction, resulting in a red shift of the main absorption peak. The long-range charge transfer emerges on the silver nanowire, and the long-distance electron-hole pairs occur near the two diagonal oxygen atoms, which stimulates the collective oscillation of the whole system, especially for the atoms on the x axis. However, the induced charge distributions at 1.72 eV are more concentrated, and most of them are located at the border of R-BTO due to the quantum confinement effect.[38] While the situation is somewhat different at 1.41 eV, the plasmon resonance of R-BTO is stronger though the relative absorption strength is much weaker, on the other hand, the long-range charge transfer of Ag nanowire is less evident though the frequency of this resonance point is very close to the eigenfrequency of the Ag nanowire. The above phenomena prove that changing the positions of silver nanowires in the hybrid system can effectively regulate the position and intensity of the main absorption peak of the hybrid system.

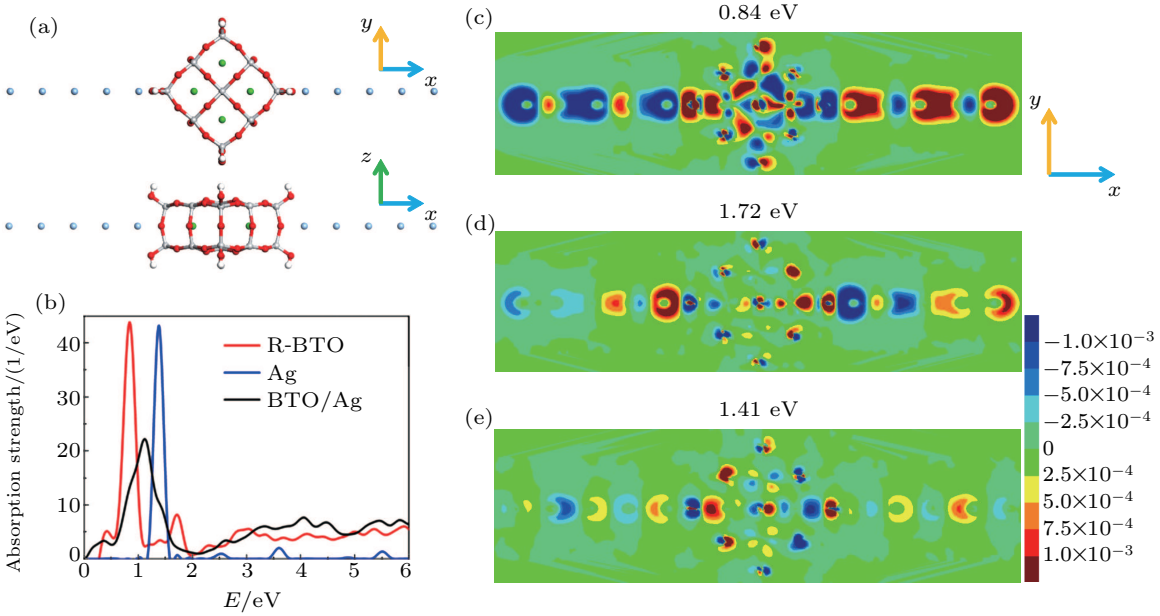


Fig. 3. (a) Top view and side view of rotated $2 \times 2 \times 1$ BTO–QDs/Ag (R-BTO/Ag) hybrid system, and geometric parameters of BTO–QDs and silver nanowire are both the same as those in Fig. 1(c). (b) Optical absorption of R-BTO/Ag, $2 \times 2 \times 1$ BTO–QDs/Ag and silver nanowire. Fourier transformations of the induced charge density distribution of R-BTO/Ag at resonance points of (c) 0.84 eV, (d) 1.72 eV, and (e) 1.41 eV, respectively.

3.3. Absorption spectrum and plasmons of thickened BTO–QDs/Ag system

To further tune the absorption spectrum and plasmons, a properly enlarged structure is taken into consideration. Figure 4(a) shows the geometric parameters of the thickened BTO–QDs/Ag hybrid system. Note that the length of 'a', length of 'b', and

length of 'h' are approximately equal, thus the separate $2\times2\times2$ BTO–QDs have a property of threefold degeneracy. Figure 4(b) displays that in the low-energy range, the absorption range of $2\times2\times2$ BTO–QDs/Ag (red curve) system is broadened, but the relative absorption strength decreases as compared with that of $2\times2\times2$ BTO–QDs/Ag system (black curve). Three peaks emerge in this range at 0.51, 0.90, 1.38 eV, respectively, and the introduction of silver nanowire is responsible for this phenomenon, for the position of silver nanowire breaks the threefold degeneracy of separate $2\times2\times2$ BTO–QDs/Ag system.

Figures 4(c)– 4(e) show the induced charge distributions of three resonance points. The comparison among these three figures shows that the hybrid system clearly presents three distinct oscillation modes at these three peaks in spite of the difference in electron density value, which proves the above-mentioned peak splitting phenomenon from the side. It is noteworthy that the best plasmon resonance phenomenon occurs at the peak of 1.38 eV, the secondary peak, as shown in Fig. 4(e), since this resonance energy point is nearly equivalent to the eigenfrequency of silver nanowire (1.37 eV). It turns out that changing the thickness can also regulate the photoelectric properties of BTO–QDs/Ag hybrid system under the same length and width. The thickening operation can effectively split the absorption peak of the hybrid system.

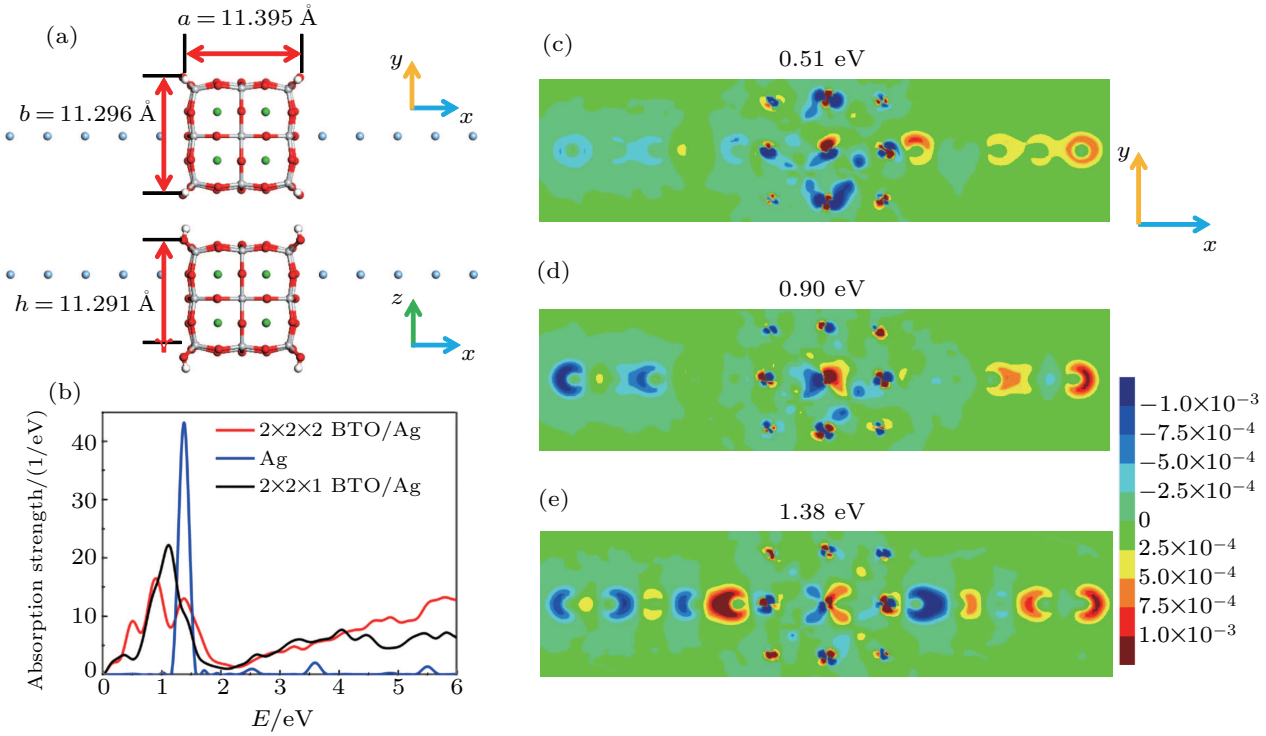


Fig. 4. (a) Top view and side view of $2\times2\times1$ BTO–QDs/Ag hybrid system. (b) Optical absorption of $2\times2\times1$ BTO–QDs/Ag, $2\times2\times1$ BTO–QDs/Ag, and silver nanowire. Fourier transformations of induced charge density distributions of $2\times2\times1$ BTO–QDs/Ag at resonance points of (c) 0.51 eV, (d) 0.90 eV, and (e) 1.38 eV, respectively.

3.4. Absorption spectrum of rotated thickened BTO–QDs/Ag system

Considering that both a rotation and thickening operation can effectively regulate the photoelectric properties of BTO–QDs/Ag hybrid system, we try to utilize both operations to observe its regulation. Figure 5(a) shows a top view and a side view of a rotated $2\times2\times2$ BTO–QDs/Ag hybrid system. The geometric parameters are all the same as those in Fig. 4(a). But there exist some differences, the separate rotated $2\times2\times2$ BTO–QDs are only twofold degenerate along the x and y direction, because the geometric length in the z direction is different from that in the x or y direction. Figure 5(b) shows the absorption spectra of rotated $2\times2\times2$ BTO–QDs/Ag hybrid system (red curve), and also the spectra of $2\times2\times2$ BTO–QDs/Ag (black curve) and rotated $2\times2\times1$ BTO–QDs/Ag (blue curve) for comparison. The phenomena corresponding to the two operations mentioned in Subsections 3.2 and 3.3 indeed coincide. Comparing the red curve with the black curve, the absorption enhancement in the low-energy region does happen after the rotation operation. While comparing the red curve with the blue curve, the main peak splits into two peaks after the thickening operation. The above phenomena prove that these two methods are indeed effective ways to regulate the photoelectric properties of BTO–QDs/Ag hybrid system, which paves the way for simultaneously achieving strong quantum properties, a considerable absorption intensity and a proper absorption region.

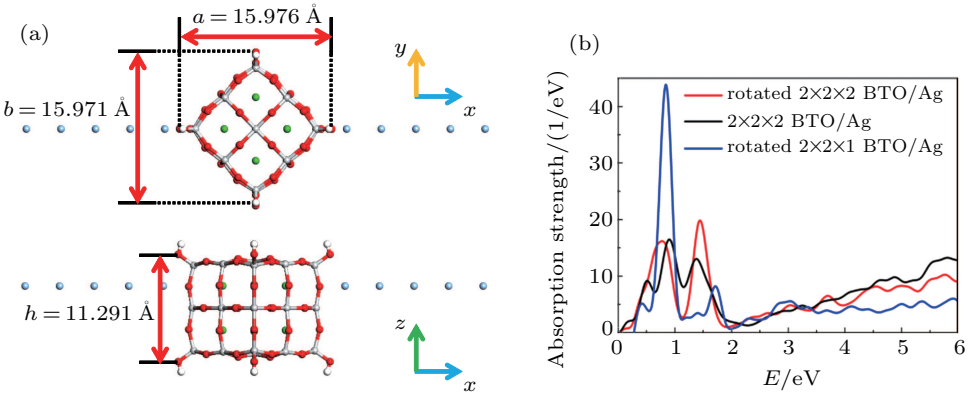


Fig. 5. (a) Top view and side view of rotated $2 \times 2 \times 2$ BTO–QDs/Ag hybrid system. (b) Optical absorption of rotated $2 \times 2 \times 2$ BTO–QDs/Ag, $2 \times 2 \times 2$ BTO–QDs/Ag, and rotated $2 \times 2 \times 1$ BTO–QDs/Ag.

4. Conclusions

Using the TDDFT, we investigate the optical response and plasmon resonance of barium titanate quantum dots coupled with silver nanowires. The silver nanowire can serve as an antenna and provides an extra electric field, resulting in the enhancement of optical properties of BTO–QDs in both low-energy and high-energy area, and the silver nanowires play a pivotal role in the collective oscillation phenomenon; in the BTO–QDs/Ag hybrid system, rotation operation is an effective method to modulate the optical response properties. The rotated BTO–QDs coupled with silver nanowire show a stronger absorption intensity and red-shifted absorption region. Thickening operation is also a useful method to tune the optical response properties of the hybrid system, and the thickened BTO–QDs coupled with silver nanowire present broader absorption range and split absorption peaks. Rotation and thickening operations can work together to further tune the optical response properties.

References

[1] Maeda K, Teramura K, Lu D, Takata T, Saito N, Inoue Y and Domen K 2006 *Nature* **440** 295

[2] L Michael M, Joël T, Tsutomu M, M Takurou N and S Henry J 2012 *Science* **338** 643

[3] Julian B, Norman P, Soo-Jin M, Robin H B, Peng G, Nazeeruddin M K and Michael G T 2013 *Nature* **499** 316

[4] Ilya G, Vincent W D, Maria T, Gaoyang G, Stein D M, Liyan W, Guannan C, Gallo E M, Akbashev A R and Davies P K 2013 *Nature* **503** 509

[5] Yang F, Lin S, Yang L, Liao J, Chen Y and Wang C Z 2017 *Mater. Res. Bull.* **96**

[6] Chen S and Shi G 2017 *Adv. Mater.* **29** 1605448

[7] Li G, Tan Z K, Di D, Lai M L, Jiang L, Lim J H, Friend R H and Greenham N C 2015 *Nano Lett.* **15** 2640

[8] Nechache R, Harnagea C, Li S, Cardenas L, Huang W, Chakrabartty J and Rosei F 2015 *Nat. Photon.* **9** 61

[9] Wang F, Grinberg I, Jiang L, Young S M, Davies P K and Rappe A M 2015 *Ferroelectrics* **483** 1

[10] Wang F, Young S M, Zheng F, Grinberg I and Rappe A M 2016 *Nat. Commun.* **7** 10419

[11] Wan D Y, Zhao Y L, Cai Y, Asmara T C, Huang Z, Chen J Q, Hong J, Yin S M, Nelson C T, Motapothula M R, Yan B X, Xiang D, Chi X, Zheng H, Chen W, Xu R, Ariando, Rusydi A, Minor A M, Breese M B H, Sherburne M, Asta M, Xu Q H and Venkatesan T 2017 *Nat. Commun.* **8** 15070

[12] Zhu T, Trevisanutto P E, Asmara T C, Xu L, Feng Y P and Rusydi A 2018 *Phys. Rev. B* **98** 235115

[13] Khaledinasab A and Sabaeian M 2012 *Appl. Opt.* **51** 4176

[14] Khaledi-Nasab A, Sabaeian M, Sahrai M and Fallahi V 2014 *J. Opt.* **16** 055004

[15] And C B M, Kagan C R and Bawendi M G 2003 *Ann. Rev. Mater. Sci.* **30** 545

[16] Ramírez H Y, Flórez J and Camacho S 2015 *Phys. Chem. Chem. Phys.* **17** 23938

[17] Coe-Sullivan S, Steckel J S, Woo W K, Bawendi M G and Bulović V 2005 *Adv. Funct. Mater.* **15** 1117

[18] Xu S, Dadlani A L, Acharya S, Schindler P and Prinz F B 2016 *Appl. Surf. Sci.* **367** 500

[19] Gorbachev I A, Goryacheva I Y and Glukhovskoy E G 2016 *Bionanoscience* **6** 1

[20] Lin J H, Zhang H, Zhang B F, Zhao J, Miyamoto Y and Cheng X L 2018 *J. Phys. Chem. C* **122** 19992

[21] Song J, Li J, Li X, Xu L, Dong Y and Zeng H 2015 *Adv. Mater.* **27** 7162

[22] Jeong-Hyeok I, Chang-Ryul L, Jin-Wook L, Sang-Won P and Nam-Gyu P 2011 *Nanoscale* **3** 4088

[23] Zhang J R, Bai D L, Jin Z W, Bian H, Wang K, Sun J, Wang Q and Liu S Z 2018 *Adv. Energy Mater.* **8** 9

[24] Fons R, Osterkryger A D, Stepanov P, Gautier E, Bleuse J, Gerard J M, Gregersen N and Claudon J 2018 *Nano Lett.* **18** 6434

[25] Leschkies K S, Divakar R, Basu J, Enache-Pommer E, Boercker J E, Carter C B, Kortshagen U R, Norris D J and Aydil E S 2007 *Nano Lett.* **7** 1793

[26] Mokkapati S, Beck F J, Waele R D, Polman A and Catchpole K R 2011 *J. Phys. D: Appl. Phys.* **44** 185101

[27] Stubhan T, Krantz J, Li N, Guo F, Litzov I, Steidl M, Richter M, Matt G J and Brabec C J 2012 *Sol. Energy Mater. Sol. Cells* **107** 248

[28] Marques M A L, Castro A, Bertsch G F and Rubio A 2003 *Comput. Phys. Commun.* **151** 60

[29] Hartwigsen C, Goedecker S and Hutter J K 1998 *Phys. Rev. B* **58** 3641

[30] Delin A, Fast L, Johansson B, Eriksson O and Wills J M 1998 *Phys. Rev. B* **58** 4345

[31] Hermann and Raphaël P 1997 *J. Phys. A: Math. Gen.* **30** 3967

[32] Lu C, Nakajima N and Maruyama H 2017 *J. Phys.-Condens. Matter* **29** 045702

[33] Cupo A and Meunier V 2017 *J. Phys.-Condens. Matter* **29** 283001

[34] Li X, Zhao J and Yang J 2013 *Sci. Rep.* **3** 1858

[35] Matsuzawa N, Ishitani A, Dixon D A and Uda T 2001 *J. Phys. Chem. A* **105** 4953

[36] Zhan C G, Dixon D A, Matsuzawa N N, Ishitani A and Uda T 2003 *J. Fluor. Chem.* **122** 27

[37] Yang T C, Wei L J, Yao W C, Tso L P, Wen L T and Tsung L P 2012 *Nano Lett.* **12** 1648

[38] Miller D A B, Chemla D S, Damen T C, Gossard A C, Wiegmann W, Wood T H and Burrus C A 1984 *Phys. Rev. Lett.* **53** 2173